Published in final edited form as:

Mol Cancer Ther. 2017 November ; 16(11): 2543–2551. doi:10.1158/1535-7163.MCT-17-0110.

TDP1 is critical for the repair of DNA breaks induced by sapacitabine, a nucleoside also targeting ATM- and BRCA-deficient tumors

Muthana Al Abo[1], **Hiroyuki Sasanuma**[2], **Xiaojun Liu**[3], **Vinodh N Rajapakse**[1], **Shar-Yin Huang**[1], **Evgeny Kiselev**[1], **Shunichi Takeda**[2], **William Plunkett**[3], and **Yves Pommier**[1]

[1]Developmental Therapeutics Branch and Laboratory of Molecular Pharmacology, Center for Cancer Research, NCI, NIH, Bethesda, MD 20892, USA.

[2]Department of Radiation Genetics, Kyoto University, Graduate School of Medicine, Yoshida Konoe, Sakyo-ku, Kyoto 606-8501, Japan.

[3]Department of Experimental Therapeutics, University of Texas M. D. Anderson Cancer Center, Houston, TX 77054, USA.

Abstract

2'-*C*-cyano-2'-deoxy-1-β-D-arabino-pentofuranosylcytosine (CNDAC) is the active metabolite of the anticancer drug, sapacitabine. CNDAC is incorporated into the genome during DNA replication and subsequently undergoes beta-elimination that generates single-strand breaks with abnormal 3'-ends. Because tyrosyl-DNA phosphodiesterase 1 (TDP1) selectively hydrolyzes non-phosphorylated 3'-blocking ends, we tested its role in the repair of CNDAC-induced DNA damage. We show that cells lacking TDP1 (avian *TDP1−/−* DT40 cells and human *TDP1 KO* TSCER2 and HCT116 cells) exhibit marked hypersensitivity to CNDAC. We also identified BRCA1, FANCD2 and PCNA in the DNA repair pathways to CNDAC. Comparing CNDAC with the chemically related arabinosyl nucleoside analog, cytosine arabinoside (cytarabine, AraC) and the topoisomerase I inhibitor camptothecin (CPT), which both generate 3'-end blocking DNA lesions that are also repaired by TDP1, we found that inactivation of BRCA2 renders cells hypersensitive to CNDAC and CPT but not to AraC. By contrast, cells lacking PARP1 were only hypersensitive to CPT but not to CNDAC or AraC. Examination of *TDP1* expression in the cancer cell line databases (CCLE, GDSC, NCI-60) and human cancers (TCGA) revealed a broad range of expression of *TDP1*, which was correlated with PARP1 expression, *TDP1* gene copy number and promoter methylation. Thus, the present study identifies the importance of TDP1 as a novel determinant of response to CNDAC across various cancer types (especially non-small cell lung cancers), and demonstrates the differential involvement of BRCA2, PARP1 and TDP1 in the cellular responses to CNDAC, AraC and CPT.

Corresponding Author., Yves Pommier, Developmental Therapeutics Branch and Laboratory of Molecular Pharmacology, Center for Cancer Research, NCI, NIH, Bethesda, MD 20892, USA. Tel: 240-760-6142; Fax: 240-541-4475; pommier@nih.gov.

Keywords

Cytosine arabinoside, cytarabine; DNA damage and repair mechanisms; BRCA1, BRCA2, ATM; DNA-reactive agents; Camptothecin; Topoisomerases; DNA damage, DNA repair, and mutagenesis

INTRODUCTION

Sapacitabine is an oral prodrug of the nucleoside analog 2′-C-cyano-2′-deoxy-1-β-D-arabino-pentofuranosylcytosine (CNDAC) (Figure 1A) (1), which is currently in clinical trial for relapsed acute myeloid leukemias (AML) and myelodysplastic syndromes (MDS) (2). The inhibitory activity of CNDAC toward tumor proliferation is achieved by generation of lethal DNA breaks (1,3). Like its analog cytosine arabinoside (cytarabine, AraC; Figure 1B), CNDAC is incorporated into DNA during replication (4) (Figure 1C). Contrary to AraC, CNDAC incorporation does not result in immediate termination of replication fork progression as the cyano substitution does not arrest DNA chain elongation. CNDAC incorporaton, however, interferes with the next round of replication (3). Following its incorporation, CNDAC undergoes β-elimination driven by the electron-withdrawing nature of the cyano group in the sugar moiety of CNDAC, leading to the cleavage of the 3′-phosphodiester linkage between CNDAC and the next nucleotide with rearrangement of the terminal CNDAC nucleotide to form 2′-C-cyano-2′,3′-didehydro-2′,3′-dideoxycytidine (CNddC) (Figure 1C) (4). Unless the 3’-blocking lesion is removed and the DNA repaired before the second round of replication, the replication machinery encounters the single-stranded DNA (ssDNA) break (SSB) at the site of CNDAC incorporation (Figure 1D), and converts the SSB in a lethal double-stranded DNA (dsDNA) break (DSB) (3,4).

Cells utilize two major pathways for DSB repair: homologous recombination and non-homologous end-joining. Previous studies reported that deficiency in homologous recombination, but not in non-homologous end-joining, results in hypersensitivity to CNDAC (3). To perform homologous recombination and error free repair, cells employ the homologous DNA template present during the S- and G2-phases. During the early steps of homologous recombination, 5’-ends of broken dsDNA are resected to generate 3’-overhangs that invades the template DNA. Following which, DNA polymerases extend the ssDNA from the 3’-overhang (5). Thus, non-canonical modifications at the 3’-end of the invading ssDNA inhibit DNA polymerization, completion of DNA repair and recovery of blocked replication forks.

Tyrosyl–DNA phosphodiesterase 1 (TDP1) was discovered as the enzyme hydrolyzing the phosphodiester bond between a DNA 3′-end and a tyrosyl moiety at the 3′-end of ssDNA that results from trapped topoisomerase I (TOP1) (6–8). Consistently, TDP1−/− cells are hypersensitive to the TOP1 poisoning anticancer drugs, camptothecin (CPT) and its clinical derivatives topotecan and irinotecan (9–12). TDP1 is also critical for the repair of DNA damage induced by chain terminating anticancer and antiviral drugs, such as AraC, acyclovir, zidovudine (AZT) and abacavir (11,13,14) and by DNA alkylating agents (11) owing to its 3’-nucleosidase activity (15,16).

Based on the proposed mechanism of action of CNDAC with formation of a DNA damage intermediate (CNddC) at the 3′-end of a ssDNA break (Figure 1D), we hypothesized that TDP1 might excise CNDAC-induced 3'-blocking DNA lesions (Figure 1E and F), and that lack of TDP1 might sensitize cancer cells to CNDAC. To test this hypothesis, we utilized *wild-type* and *TDP1−/−* avian leukemia DT40 cells (11,13), and generated human *TDP1* knockout TK6 and HCT116 cells, and performed viability assays and cell cycle analyses. We also investigated the impact of other DNA repair pathways on the viability of cells treated with CNDAC using our panel of isogenic DT40 cell lines with inactivation of DNA repair pathways (17,18). Those pathways included repair defects that are known to occur in human cancers such as BRCA1, BRCA2, ATM, Fanconi Anemia (FA) and translesion synthesis (TLS) genes. Our results uncover the role of TDP1 in repairing DNA damage induced by sapacitabine and extends our understanding of the common and differential molecular determinants of therapeutics response to sapacitabine, cytarabine and camptothecin.

MATERIAL AND METHODS

Cell cultures

DT40 cells were cultured at 37°C with 5% CO2 in Roswell Park Memorial Institute (RPMI-1640) medium supplemented with 1% chicken serum (Life Technologies, Carlsbad, CA, USA), 10^{-5} M β-mercaptoethanol, 100 U/mL penicillin and 100 μg/mL streptomycin and 10% fetal bovine serum (FBS). Generation of *TDP1−/−* DT40 cells were as previously described in (11). All DT40 mutant cells that are used in this manuscript are the same cells in (17). The human lymphoblastoid cell line, TSCER2 cells (19) were grown in RPMI-1640 medium supplemented with 100 μg/mL sodium pyruvate, 100 U/mL penicillin and 100 μg/mL streptomycin and 10% fetal bovine serum (FBS) and HCT116 cells were grown in DME supplemented with 10 FBS. Both TSCER2 and HCT116 were grown at 37°C with 5% CO_2. No authentication was done by the authors.

Generation of TSCER2 *TDP1 KO* cells

To disrupt TDP1 gene, the guide RNA (5'-GCAAAGTTGGATATTGCGTT-3') was inserted into the pX330 expression vector (Addgene). For construction of the TDP1 targeting vectors, the left and right arms of the constructs were amplified from genomic DNA, respectively. The left and right arms were amplified using F1/R1 and F2/R2 primers. The resulting fragments were assembled with either *DT-ApA/NEO*^{R} or *DT-ApA/PURO*^{R} (provided from the Laboratory for Animal Resources and Genetic Engineering, Center for Developmental Biology, RIKEN Kobe, http://www.cdb.riken.jp/arg/cassette.html) having been digested with *ApaI* and *AflII* using the GeneArt Seamless cloning kit (Invitrogen, US). Nucleotides indicated by capital letters in F1 and R1 are identical with sequences upstream and downstream, respectively, of the *ApaI* site. Nucleotides indicated by capital letters in in F2 and R2 are identical with sequences upstream and downstream of the *AflII* site. Transfection was done as described previously (20). *TDP1 KO* clones were identified by genomic PCR using F3/R3 (for *NEO*^{R}) and F4/R3 (for *PURO*^{R}). The absence of *TDP1* mRNA was confirmed by RT-PCR using F5/R4 primers (Supplementary Figure 1A). Expression of GAPDH mRNA as a loading control was amplified by F6/R5.

1. F1, 5’-GCGAATTGGGTACCGGGCCaaatatcagtttatagagtggcag-3’
2. R1, 5’-CTGGGCTCGAGGGGGGGCCgaagtcatttatttaaaaacaact-3’
3. F2, 5’-TGGGAAGCTTGTCGACTTAAgaacccctcaagcattgtcatttg-3’
4. R2, 5’-CACTAGTAGGCGCGCCTTAAttggtctcgaactcctgatctcaaa-3’
5. R3, 5’-GATACTTAATTGGGAAAAGTTCAACTGTAA-3’
6. F3, 5’-AACCTGCGTGCAATCCATCTTGTTCAATGG-3’
7. F4, 5’-GTGAGGAAGAGTTCTTGCAGCTCGGTGA-3’
8. F5, GAAGAAGCCAATCCTGCTTGTGCATGGTGA
9. R4, TTTGTTTCAGAGAGATCGTGCTTGTGAATG
10. F6, GCGCCAGTAGAGGCAGGGATGATGT
11. R5, GCGCCAGTAGAGGCAGGGATGATGT

Generation of HCT116 *TDP1 KO* cells

TDP1 knockout in HCT116 cells were generated by CRISPR genome editing method targeting exon5 of *TDP1* (Target site: GTTTAACTACTGCTTTGACGTGG). Plasmid pX330 (21) with the cloned-in target site sequence were co-transfected with a *Puro*-resistance gene flanked by homology arms up-stream and down-stream of the target site. Transfected cells were selected with 1 μg/mL of puromycin 72 hours post initial transfection for cells with puro-resistance gene recombined into at least one copy of the target site. Established clones from single cell were subsequently screened by biochemical assay (3’-phosphotyrosyl cleavage activity) to identify clones without detectable TDP1 activity (Supplementary Figure 1A).

Measurement of cellular sensitivity to DNA-damaging drugs

To measure the sensitivity of cells to CNDAC (obtained from Dr. William Plunkett, the University of Texas MD Anderson Cancer Center), AraC (Sigma-Aldrich, St. Louis, MO, USA), or CPT (obtained from the Developmental Therapeutics Program (DCTD, NCI)), 750 DT40 cells were seeded in 96-well white plate (final volume 150 μl/well) from Perkin Elmer Life Sciences (Waltham, MA, USA) with the indicated drugs at 37°C. After 72 h, cells were assayed in triplicates with the ATPlite 1-step kit (PerkinElmer, Waltham, MA, USA). Briefly, ATPlite solution was added to each well (150 μl for DT40 cells). After 5 minute treatments, luminescence intensity was measured by Envision 2104 Multilabel Reader from Perkin Elmer Life Sciences (Waltham, MA, USA). Signal intensities of untreated cells were set as 100%.

Cell cycle analyses

DT40 cells were continuously exposed to fixed concentrations of CNDAC at 37°C for 12 or 24 hours. Harvested cells were fixed with 70% ethanol before re-suspension in phosphate-buffered saline containing 50μg/ml propidium iodide. Samples were then subjected to analysis on an LSRFortessa cell analyzer from BD Biosciences (Franklin Lakes, NJ, USA).

TDP1 activity and biochemical assays

The assay was done as described in (22). A 5'-[^{32}P]-labeled single-stranded DNA oligonucleotide containing a 3'-phosphotyrosine (N14Y, 5′-GATCTAAAAGACTT**Y**, Midland Certified Reagents Company) was incubated at 1 nM with whole cell extract for 15 min at room temperature in buffer containing 50 mM Tris HCl, pH 7.5, 80 mM KCl, 2 mM EDTA, 1 mM DTT, 40 μg/mL BSA, and 0.01% Tween-20. Reactions were terminated by the addition of 1 volume of gel loading buffer [99.5% (v/v) formamide, 5 mM EDTA, 0.01% (w/v) xylene cyanol, and 0.01% (w/v) bromophenol blue]. Samples were subjected to a 16% denaturing PAGE. Gels were dried and exposed to a PhosphorImager screen (GE Healthcare). Gel images were scanned using a Typhoon™ FLA 9500 (GE Healthcare).

Colony survival assay

To perform survival assay using TSCER2 cells, we seeded 75 cells in each well of 6-well plate in methylcellulose medium with or without CNDAC drug. We prepared the methylcellulose medium as described in (23). After incubating the cells for 12 days at 37°C with 5% CO2, we counted the number of colonies in each well. To perform survival assay using HCT116 cells, cells were incubated in DMEM medium and next day (after cells adhered to the plate) the medium was aspirated and new media with or without CNDAC were added to the cell. After 15-day incubation, the medium was removed and colonies were fixed on the plate with methanol for 5 minutes. The methanol was removed and the colonies were rinsed with phosphate-buffered saline and then stained for 10 minutes with 0.5% crystal violet in water. After the removal of the crystal violet solution, cells were washed again with phosphate-buffered saline and left to dry. The number of colonies were in each well were counted. To calculate the survival ratios, we divided the number of colonies in wells with CNDAC drugs by the number of colonies in wells which contain medium only.

TOP1 cleavage complex detection by Immuno Complex of Enzyme (ICE) Bioassay

ICE bioassay was performed as described (24,25). Briefly, Pellet of 2X10^6 TK6 cells were lysed in 2 ml 1% Sarkosyl. Cell lysates were added on the top of 1.82, 1.72, 1.50 and 1.45 densities of CsCl solutions. After centrifuging the tubes at 30700 rpm at room temperature for 20 hours, 1 ml fractions were collected from the bottom of the tubes. 100 μl of each fraction were mixed with 100 μl of 25 mM sodium phosphate buffer. Using a slot-blot vacuum, each fraction solutions were blotted onto millipore pvdf membranes. To detect TOP1cleavage complex (TOP1cc), 5% milk in PBS (phosphate-buffered saline) for 1 hour at RT was used for blocking which was followed by incubation for 2 hours at room temperature with 5% milk containing TOP1 antibody (#556597; BD Biosciences, San Jose, CA) (1:1000 dilution). Membrane was washed with PBST (phosphate-buffered saline, Tween-20 0.05%) 3 times for 5 minutes. Horseradish peroxidase–conjugated goat anti-mouse (1:5000 dilution) antibody (Amersham Biosciences, Piscataway, NJ) in 1% milk in PBS was added to the membrane and incubated for 1 hour at RT. After washing the membrane with PBST 5 times for 5 minutes, TOP1 was detected by enhanced chemiluminescence detection kit (Thermo Scientific, Rockford, IL).

Genomic and bioinformatics analyses

Genomic analyses were performed using rCellMiner (26) based on the genomic databases from the ~ 1000 cancer cell line databases of the Cancer Cell Line Encyclopedia (CCLE; http://www.broadinstitute.org/ccle/) (27) and the Genomics of Drug Sensitivity in Cancer (GDSC; http://www.cancerrxgene.org/) (28).

RESULTS

TDP1−/− cells are hypersensitive to CNDAC

To examine the potential impact of *TDP1* gene deletion on cell survival, we treated TDP1 proficient (*wild-type*) and TDP1 deficient (*TDP1−/−*) chicken DT40 cells for 72 hours with increasing concentrations of CNDAC and measured cell viability. Elimination of *TDP1* (*TDP1−/−*) severely reduced cell viability (Inhibitory Concentration that kills 90% of cells (IC90) was 31 nM in *TDP1−/−* vs 138 nM in *wild-type* cells) (Figure 2A). To further establish the causality between TDP1 expression and CNDAC activity, we tested whether human TDP1 (hTDP1) can rescue the hypersensitivity phenotype of *TDP1−/−* cells. Accordingly, expression of human TDP1 (hTDP1) in the *TDP1−/−* cells enhanced cell viability (Figure 2A). The partial complementation by human TDP1 could be due to species differences.

To further understand the differential effects of CNDAC in TDP1-proficient and deficient cells, we used cell sorting (FACS) to measure cell cycle distribution and DNA content of CNDAC-treated and untreated cells. When DNA damage overwhelms the cell repair capacity, apoptosis ensues, which is indicated by genomic DNA fragmentation. Therefore, by measuring DNA content while performing cell cycle analysis, we could estimate the apoptotic fraction (29). Because CNDAC causes DSBs during the second round of replication, analyses were performed after 24 hours, which represents 3 rounds of replication for the fast growing DT40 cells. A significant fraction of apoptotic cells (28%) appeared as sub-G1 population in the *TDP1−/−* cells treated with CNDAC (Figure 2B–C). In contrast, sub-G1 populations of *wild-type* cells were comparable between treated and untreated cells and the *TDP1−/−*+hTDP1 cells showed significantly less sub-G1 fraction (16.4%) compared to *TDP1−/−* cells (Figure 2B and C). We also observed accumulation of G2 fraction with CNDAC treatment, which represents DNA-damaged cells during S-phase. When we treated the cells with lower concentrations of CNDAC for only 12 hours, cell-cycle analysis showed G2 accumulation (Figure 2D and E), reflecting replicative DNA damage induced by CNDAC.

Taken together, the cell viabilities and FACS analyses experiments demonstrate that deletion of TDP1 renders cells hypersensitive to CNDAC, implying the role of TDP1 in the repair of CNDAC-induced DNA damage.

CRISPR *TDP1* Knockout human TSCER2 lymphoblastoid and HCT116 colon carcinoma cells are hypersensitive to CNDAC

To confirm our findings in human cells, we knocked out the *TDP1* gene in human lymphoblastoid TSCER2 and colon carcinoma HCT116 cells using CRISPR-cas9

(Supplementary Figure 1A and B). We validated the efficient knockout of *TDP1* by performing biochemical TDP1 assays in cellular extracts from parental cells (*wild-type*) or *TDP1* knockout (*TDP1 KO*) cells (Figure 3A and B) (11). Next, the cytotoxicity of CNDAC was evaluated in the TSCER2 and HCT116 *TDP1 KO* cells in comparison to the matching parental *wild-type* cells. Colony survival assays using media containing increasing concentration of CNDAC showed that *TDP1 KO* cells were significantly more sensitive than the *wild-type* cells (Figure 3C and D). These results establish the importance of TDP1 for the repair of CNDAC-induced DNA damage and in the tolerance to CNDAC treatment in human cells.

It has been established that DNA nicks can trap TOP1 and result in TOP1-DNA cleavage complexes (TOP1cc) (30,31). To answer the question whether the hypersensitivity of *TDP1 KO* could be caused by the ability of CNDAC to trap TOP1cc, we performed ICE bioassays to detect TOP1cc after CNDAC treatment. Repeated experiments failed to detect TOP1cc after CNDAC treatment under conditions where CPT, which was used as positive control, induced signal for TOP1cc (Figure 3E). The results of these experiments favor the model shown in Figure 1, in which TDP1 repairs CNDAC-induced nicks by its 3'-end nucleosidase activity.

Deletions of BRCA1, BRCA2, FANCD2, or ATM sensitize cells to CNDAC

To uncover additional repair factors/pathways involved in CNDAC-induced DNA damage, we took a genetic approach using our library of DT40 cells that are deficient in various DNA repair pathways (17,18), including homologous recombination (HR), non-homologous end-joining (NHEJ), Fanconi anemia (FA) and translesion DNA synthesis (TLS) using the DNA polymerase mutant cofactor PCNAK164 (ubiquitin site mutant).

In agreement with recent reports (1,3), we observed hypersensitivity in *BRCA2, ATM* and *XRCC3* knockout cells (Figure 4B). We also observed hypersensitivity in *BRCA1*, *FANCD2* knockout and *PCNA* (*PCNA-/K164R*) mutant cells (Figure 4A and B). By contrast, XRCC6 (Ku70) deficient cells showed no hypersensitivity to CNDAC (Figure 4B). These results are consistent with replication damage induction by CNDAC and with their repair by homologous recombination rather than end-joining. Although TDP1 has been reported to function in association with PARP1 (32), *PARP1* knockout cells were not hypersensitive to CNDAC. This result indicates that TDP1 functions independently of PARP in the repair of CNDAC-induced damage. This is notably different from the reported PARP1-TDP1 coupling for the repair of TOP1-induced DNA damage (32,33).

Differential roles of TDP1, PARP1 and BRCA2 for the repair of 3'-end DNA lesions induced by CNDAC, AraC and CPT

In addition to CNDAC, TDP1 has been shown to excise a broad range of 3'-end blocking lesions (11,13,15,16,34) including the chain terminator nucleoside analog AraC and the TOP1 poison CPT, which both generate 3'-end lesions but with different biochemical characteristics. To determine the common and differential repair pathways associated with TDP1, we compared the involvement of PARP1 and BRCA2 in the cellular responses to AraC and CPT in parallel with CNDAC. Figure 5 demonstrates notable differences.

Consistent with previous reports, TDP1 knockout cells are hypersensitive to both AraC and CPT (9,10,13) in addition to being hypersensitive to CNDAC, consistent with the broad role of TDP1 in the cleansing of 3'-end blocking lesions. Regarding BRCA2, Figure 5 shows that *BRCA2* knockout cells are hypersensitive to CNDAC and CPT but not to AraC. These results are consistent with the conclusion that the DNA lesions generated by CNDAC and CPT are DSBs in S-phase, which are repaired by homologous recombination. They also demonstrate that AraC-induced damage is not repaired via HR. In addition, while PARP1 knockout cells are hypersensitive CPT (35), they are not hypersensitive to CNDAC or AraC (Figure 5). This result shows that TDP1 can function independently of PARP1 in response to CNDAC- or AraC-induced DNA damages. Our findings highlight the differential cellular responses to 3'-end blocking anticancer drugs and the involvement of different repair factors and pathways.

TDP1 expression range in cancer cell lines and in cancer samples from the TCGA

Because of the emerging importance of TDP1 as a potential determinant of response to an increasing number of therapeutically relevant DNA damaging agents, we examined *TDP1* expression in publicly available cancer genomic databases.

In the ~ 1000 cancer cell line databases of the Cancer Cell Line Encyclopedia (CCLE) (27) and the Genomics of Drug Sensitivity in Cancer (GDSC) (28) projects, *TDP1* expression varies broadly across cell lines and tissues of origin (Figure 6A–D y axis, and Supplementary Figure 2A). This variation is due, in part to amplifications and deletions (CNV, copy number variation) of the *TDP1* gene locus (Figure 6A–C) on chromosome 14q32.11. Moreover, leukemia and blood cancers tend to have high *TDP1* expression (Figure 6B) while non-small cell lung cancers (NSCLC) have the broadest *TDP1* expression range with some cells having background (no significant) *TDP1* expression (Figure 6C and Supplementary Figure 2A). In the NSCLC cell lines, we found that lack of *TDP1* expression is also driven by promoter hypermethylation (Figure 6D) (36).

Similarly, in The Cancer Genome Atlas (TCGA) database, *TDP1* expression varies widely (Figure 6E and Supplementary Figure 2B), and the NSCLC samples show the broadest *TDP1* expression range with some cancers having insignificant *TDP1* mRNA (Figure 6E). By contrast, acute myelocytic leukemia (AML) samples show consistently high *TDP1* expression (Figure 6E and Supplementary Figure 2B). Together, these genomic analyses demonstrate that *TDP1* exhibits a wide range of expression, most notably in NSCLC, and that *TDP1* expression variation correlates positively with *TDP1* gene copy number variation (Figure 6A–C) and negatively with *TDP1* promoter methylation (Figure 6D).

DISCUSSION

Here we report evidence supporting that TDP1 repairs the DNA damage induced by CNDAC, the active metabolite of the novel anticancer drug sapacitabine, which supports the proposed mechanism of DNA damage by sapacitabine (Figure 1). We show that the avian leukemia *TDP1* knockout DT40 cells are almost as hypersensitive as BRCA1- or BRCA2-deficient cells to CNDAC compared to wild-type cells (Figures 2 and 4), and that they are similarly hypersensitive as cells defective for ATM or FANCD2 (Figure 4). We also expand

these findings by showing that human TSCER2 lymphoblastoid and HCT116 colon carcinoma *TDP1* knockout cells are hypersensitive to CNDAC as well (Figure 3), and that complementation of DT40 *TDP1* knockout cells with human *TDP1* rescues the viability of those cells in response to CNDAC (Figure 2).

The mode of action of widely used anticancer nucleoside analogs, such as cytarabine, is to block replication by incorporating a modified nucleotide at the 3′-end of DNA during replication chain elongation. Previous results (11,13) as well as results shown here demonstrate that TDP1 plays a critical role in processing these abnormal 3′-ends, which ultimately enables the repair process. Although the 3'-end blocking anticancer drugs tested here generate 3'-end lesions that require TDP1 (Figure 5), additional repair pathways downstream to TDP1 vary. Indeed, we observed differential requirement of BRCA2 and PARP1 for CNDAC, CPT or AraC. This is likely due to the fact that these agents cause DNA lesions that relate to replication in different ways: 1) CNDAC and CPT damage the DNA template whereas AraC damages the newly synthesized DNA; 2) CPT blocks replication ahead of replication forks, while AraC terminates the elongation of replication forks and CNDAC stops replication by breaking the template; 3) CPT and CNDAC cause replication-mediated double-stranded DNA breaks, which is not the case of AraC; and 4) CNDAC induces ssDNA nicks only behind the replication fork whereas CPT generates TOP1 cleavage complexes ahead of replication forks.

Recently, using Chinese hamster cells, it was reported that the combination of CNDAC with PARP1 inhibitors, olaparib, rucaparib, and talazoparib was synergistic in HR-deficient (BRCA2-, XRCC3- and RAD51D-deficient cells) but not in wild-type cells at relatively lower concentrations (37). Our results showing no impact of PARP inactivation on CNDAC cytotoxicity in wild-type cells is consistent with this previous report.

Understanding the specific repair pathways for new drugs is critical for their effective development and precise use as anticancer agents. It is notable that the pathways that repair sapacitabine-induced DNA damage (BRCA1, BRCA2, ATM and FA) have been found defective in a significant number of cancers, suggesting they could be used for synthetic lethality approaches. Scoring TDP1 deficiency in cancers could be included in the screening of tumors in addition to ATM, HR and FA genes mutations for choosing sapacitabine as a therapeutic option beyond leukemia and myelodysplastic syndromes.

In this study, we extend our initial finding that TDP1 was found inactivated in two of the lung cancer cell lines of the NCI-60 (36) by showing lowest *TDP1* expression in NSCLC cancer cell lines and tumor samples, and establishing that both gene copy number defects and promoter hypermethylation cause such defective expression. We also found a broad range of expression of *TDP1* across cancer cells (Figure 6 and Supplemental Figure 2). Further analyses (26) in the 1000 cell lline collections [CCLE (27) and GDSC) (28)] show that *TDP1* expression is highly significantly correlated with other DNA repair genes including *PARP1, BRCA2, BRCA1, FANCM* and *BLM* and DNA replication genes including *POLD1, POLE2* and *ORC1*, suggesting the coordinated activation of the DNA repair and replication pathways in cancer cells.

Supplementary Material

Refer to Web version on PubMed Central for supplementary material.

Acknowledgments

Financial support.

Our studies are supported by the Intramural Program of the National Cancer Institute, Center for Cancer Research [Z01 BC006150] to YP and MA; NIH-NCI [R01 CA028596] to WP and XL; and a Grant-in-Aid from the Ministry of Education, Science, Sport and Culture to ST [KAKENHI 16H06306], and HS [KAKENHI 16H02953]

References

1. Liu XJ, Nowak B, Wang YQ, Plunkett W. Sapacitabine, the prodrug of CNDAC, is a nucleoside analog with a unique action mechanism of inducing DNA strand breaks. Chin J Cancer. 2012; 31(8): 373–80. [PubMed: 22739266]
2. Kantarjian H, Garcia-Manero G, O'Brien S, Faderl S, Ravandi F, Westwood R, et al. Phase I clinical and pharmacokinetic study of oral sapacitabine in patients with acute leukemia and myelodysplastic syndrome. J Clin Oncol. 2010; 28(2):285–91. [PubMed: 19933907]
3. Liu X, Wang Y, Benaissa S, Matsuda A, Kantarjian H, Estrov Z, et al. Homologous recombination as a resistance mechanism to replication-induced double-strand breaks caused by the antileukemia agent CNDAC. Blood. 2010; 116(10):1737–46. [PubMed: 20479284]
4. Azuma A, Huang P, Matsuda A, Plunkett W. 2'-C-cyano-2'-deoxy-1-beta-D-arabino-pentofuranosylcytosine: a novel anticancer nucleoside analog that causes both DNA strand breaks and G(2) arrest. Mol Pharmacol. 2001; 59(4):725–31. [PubMed: 11259616]
5. Krejci L, Altmannova V, Spirek M, Zhao X. Homologous recombination and its regulation. Nucleic Acids Res. 2012; 40(13):5795–818. [PubMed: 22467216]
6. Dexheimer TS, Stephen AG, Fivash MJ, Fisher RJ, Pommier Y. The DNA binding and 3'-end preferential activity of human tyrosyl-DNA phosphodiesterase. Nucleic Acids Res. 2010; 38(7): 2444–52. [PubMed: 20097655]
7. Pouliot JJ, Yao KC, Robertson CA, Nash HA. Yeast gene for a Tyr-DNA phosphodiesterase that repairs topoisomerase I complexes. Science. 1999; 286(5439):552–5. [PubMed: 10521354]
8. Liu C, Pouliot JJ, Nash HA. Repair of topoisomerase I covalent complexes in the absence of the tyrosyl-DNA phosphodiesterase Tdp1. Proc Natl Acad Sci U S A. 2002; 99(23):14970–5. [PubMed: 12397185]
9. El-Khamisy SF, Saifi GM, Weinfeld M, Johansson F, Helleday T, Lupski JR, et al. Defective DNA single-strand break repair in spinocerebellar ataxia with axonal neuropathy-1. Nature. 2005; 434(7029):108–13. [PubMed: 15744309]
10. Miao ZH, Agama K, Sordet O, Povirk L, Kohn KW, Pommier Y. Hereditary ataxia SCAN1 cells are defective for the repair of transcription-dependent topoisomerase I cleavage complexes. DNA repair. 2006; 5(12):1489–94. [PubMed: 16935573]
11. Murai J, Huang SY, Das BB, Dexheimer TS, Takeda S, Pommier Y. Tyrosyl-DNA phosphodiesterase 1 (TDP1) repairs DNA damage induced by topoisomerases I and II and base alkylation in vertebrate cells. J Biol Chem. 2012; 287(16):12848–57. [PubMed: 22375014]
12. Meisenberg C, Gilbert DC, Chalmers A, Haley V, Gollins S, Ward SE, et al. Clinical and Cellular Roles for TDP1 and TOP1 in Modulating Colorectal Cancer Response to Irinotecan. Mol Cancer Ther. 2015; 14(2):575–85. [PubMed: 25522766]
13. Huang SY, Murai J, Dalla Rosa I, Dexheimer TS, Naumova A, Gmeiner WH, et al. TDP1 repairs nuclear and mitochondrial DNA damage induced by chain-terminating anticancer and antiviral nucleoside analogs. Nucleic Acids Res. 2013; 41(16):7793–803. [PubMed: 23775789]
14. Tada K, Kobayashi M, Takiuchi Y, Iwai F, Sakamoto T, Nagata K, et al. Abacavir, an anti-HIV-1 drug, targets TDP1-deficient adult T cell leukemia. Sci Adv. 2015; 1(3):e1400203. [PubMed: 26601161]

15. Interthal H, Chen HJ, Champoux JJ. Human Tdp1 cleaves a broad spectrum of substrates including phosphoamide linkages. J Biol Chem. 2005 Oct 28.280:36518–28. [PubMed: 16141202]
16. Zhou T, Lee JW, Tatavarthi H, Lupski JR, Valerie K, Povirk LF. Deficiency in 3'-phosphoglycolate processing in human cells with a hereditary mutation in tyrosyl-DNA phosphodiesterase (TDP1). Nucleic Acids Res. 2005; 33(1):289–97. [PubMed: 15647511]
17. Maede Y, Shimizu H, Fukushima T, Kogame T, Nakamura T, Miki T, et al. Differential and common DNA repair pathways for topoisomerase I- and II-targeted drugs in a genetic DT40 repair cell screen panel. Mol Cancer Ther. 2014; 13(1):214–20. [PubMed: 24130054]
18. Murai J, Huang S-yN, Das BB, Renaud A, Zhang Y, Doroshow JH, et al. Trapping of PARP1 and PARP2 by Clinical PARP Inhibitors. Cancer Research. 2012; 72(21):5588–99. [PubMed: 23118055]
19. Honma M, Izumi M, Sakuraba M, Tadokoro S, Sakamoto H, Wang W, et al. Deletion, rearrangement, and gene conversion; genetic consequences of chromosomal double-strand breaks in human cells. Environ Mol Mutagen. 2003; 42(4):288–98. [PubMed: 14673874]
20. Hoa NN, Akagawa R, Yamasaki T, Hirota K, Sasa K, Natsume T, et al. Relative contribution of four nucleases, CtIP, Dna2, Exo1 and Mre11, to the initial step of DNA double-strand break repair by homologous recombination in both the chicken DT40 and human TK6 cell lines. Genes Cells. 2015; 20(12):1059–76. [PubMed: 26525166]
21. Cong L, Ran FA, Cox D, Lin S, Barretto R, Habib N, et al. Multiplex genome engineering using CRISPR/Cas systems. Science. 2013; 339(6121):819–23. [PubMed: 23287718]
22. Das BB, Dexheimer TS, Maddali K, Pommier Y. Role of tyrosyl-DNA phosphodiesterase (TDP1) in mitochondria. Proc Natl Acad Sci U S A. 2010; 107(46):19790–5. [PubMed: 21041670]
23. Tsuda M, Terada K, Ooka M, Kobayashi K, Sasanuma H, Fujisawa R, et al. The dominant role of proofreading exonuclease activity of replicative polymerase epsilon in cellular tolerance to cytarabine (Ara-C). Oncotarget. 2017
24. Pourquier P, Takebayashi Y, Urasaki Y, Gioffre C, Kohlhagen G, Pommier Y. Induction of topoisomerase I cleavage complexes by 1-beta -D-arabinofuranosylcytosine (ara-C) in vitro and in ara-C-treated cells. Proc Natl Acad Sci U S A. 2000; 97(4):1885–90. [PubMed: 10677551]
25. Subramanian D, Kraut E, Staubus A, Young DC, Muller MT. Analysis of topoisomerase I/DNA complexes in patients administered topotecan. Cancer Res. 1995; 55(10):2097–103. [PubMed: 7743509]
26. Luna A, Rajapakse VN, Sousa FG, Gao J, Schultz N, Varma S, et al. rcellminer: exploring molecular profiles and drug response of the NCI-60 cell lines in R. Bioinformatics. 2015
27. Barretina J, Caponigro G, Stransky N, Venkatesan K, Margolin AA, Kim S, et al. The Cancer Cell Line Encyclopedia enables predictive modelling of anticancer drug sensitivity. Nature. 2012; 483(7391):603–307. [PubMed: 22460905]
28. Garnett MJ, Edelman EJ, Heidorn SJ, Greenman CD, Dastur A, Lau KW, et al. Systematic identification of genomic markers of drug sensitivity in cancer cells. Nature. 2012; 483(7391): 570–5. [PubMed: 22460902]
29. Umansky SR, Korol BA, Nelipovich PA. In vivo DNA degradation in thymocytes of gamma-irradiated or hydrocortisone-treated rats. Biochimica et biophysica acta. 1981; 655(1):9–17. [PubMed: 7260092]
30. Pourquier P, Pilon A, Kohlhagen G, Mazumder A, Sharma A, Pommier Y. Trapping of mammalian topoisomerase I and recombinations induced by damaged DNA containing nicks or gaps: importance of DNA end phosphorylation and camptothecin effects. J Biol Chem. 1997; 272:26441–7. [PubMed: 9334220]
31. Huang SN, Williams JS, Arana ME, Kunkel TA, Pommier Y. Topoisomerase I-mediated cleavage at unrepaired ribonucleotides generates DNA double-strand breaks. Embo J. 2016 In press.
32. Das BB, Huang SY, Murai J, Rehman I, Ame JC, Sengupta S, et al. PARP1-TDP1 coupling for the repair of topoisomerase I-induced DNA damage. Nucleic Acids Res. 2014; 42:4435–49. [PubMed: 24493735]
33. Murai J, Marchand C, Shahane SA, Sun H, Huang R, Zhang Y, et al. Identification of novel PARP inhibitors using a cell-based TDP1 inhibitory assay in a quantitative high-throughput screening platform. DNA repair. 2014; 21:177–82. [PubMed: 24794403]

34. Zhou T, Akopiants K, Mohapatra S, Lin PS, Valerie K, Ramsden DA, et al. Tyrosyl-DNA phosphodiesterase and the repair of 3'-phosphoglycolate-terminated DNA double-strand breaks. DNA repair. 2009; 8(8):901–11. [PubMed: 19505854]

35. Zhang YW, Regairaz M, Seiler JA, Agama KK, Doroshow JH, Pommier Y. Poly(ADP-ribose) polymerase and XPF-ERCC1 participate in distinct pathways for the repair of topoisomerase I-induced DNA damage in mammalian cells. Nucleic Acids Res. 2011; 39:3607–20. [PubMed: 21227924]

36. Gao R, Das BB, Chatterjee R, Abaan OD, Agama K, Matuo R, et al. Epigenetic and genetic inactivation of tyrosyl-DNA-phosphodiesterase 1 (TDP1) in human lung cancer cells from the NCI-60 panel. DNA repair. 2014; 13:1–9. [PubMed: 24355542]

37. Liu X, Jiang Y, Nowak B, Hargis S, Plunkett W. Mechanism-Based Drug Combinations with the DNA Strand-Breaking Nucleoside Analog CNDAC. Mol Cancer Ther. 2016; 15(10):2302–13. [PubMed: 27474148]

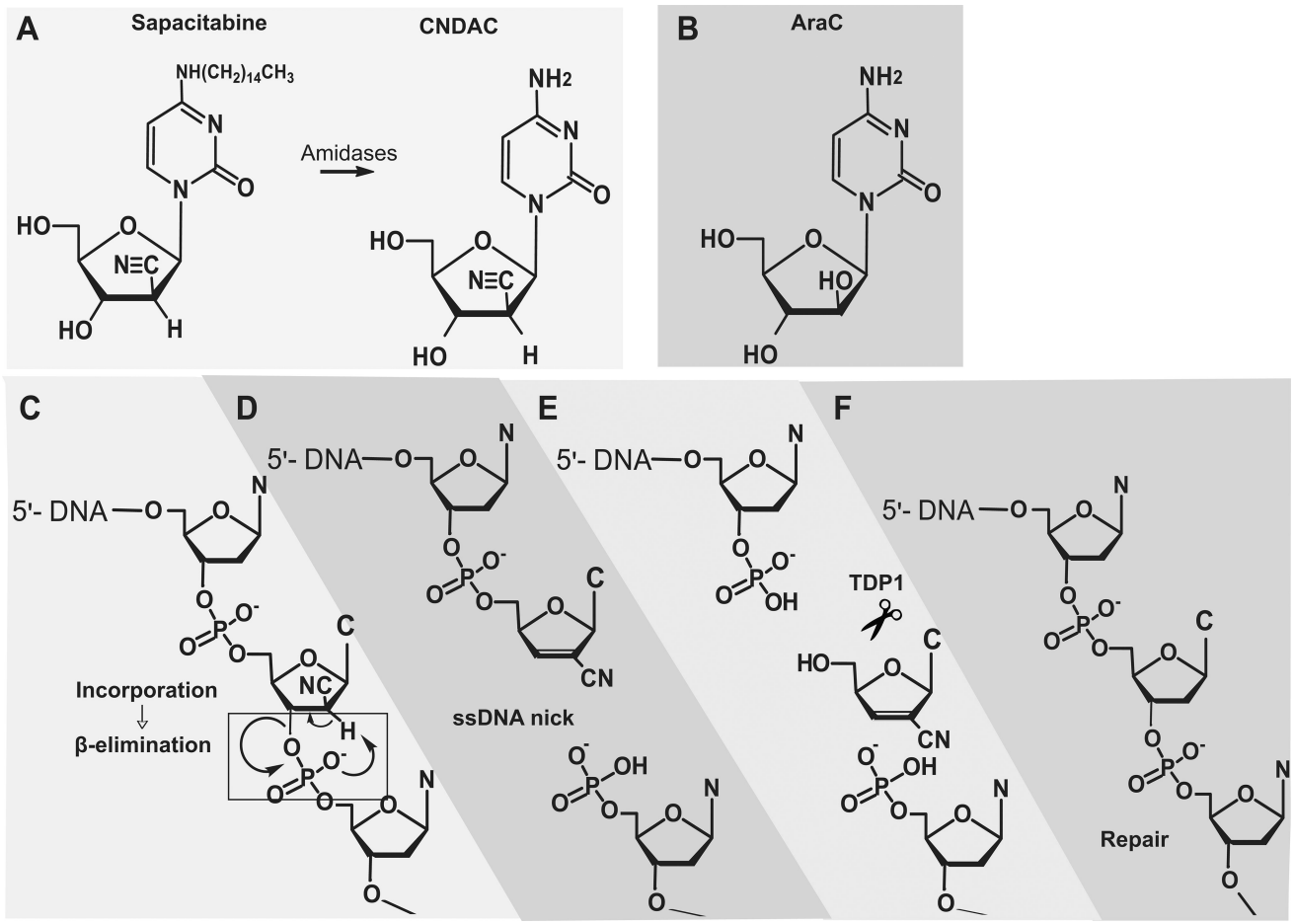

Figure 1.

Illustration of the involvement of TDP1 in the repair of CNDAC-induced DNA damage. (A) Amidase converts sapacitabine to CNDAC. (B) Chemical structure of cytosine arabinoside (cytarabine; AraC). (C-D) Proposed mechanism for the generation of ssDNA nicks by β-elimination of incorporated CNDAC (highlighted in the box). (E) Excision by TDP1 (shown as scissors) of the 3'-blocking lesion generated by CNDAC. (F) Repair by gap filing independently of PARP1.

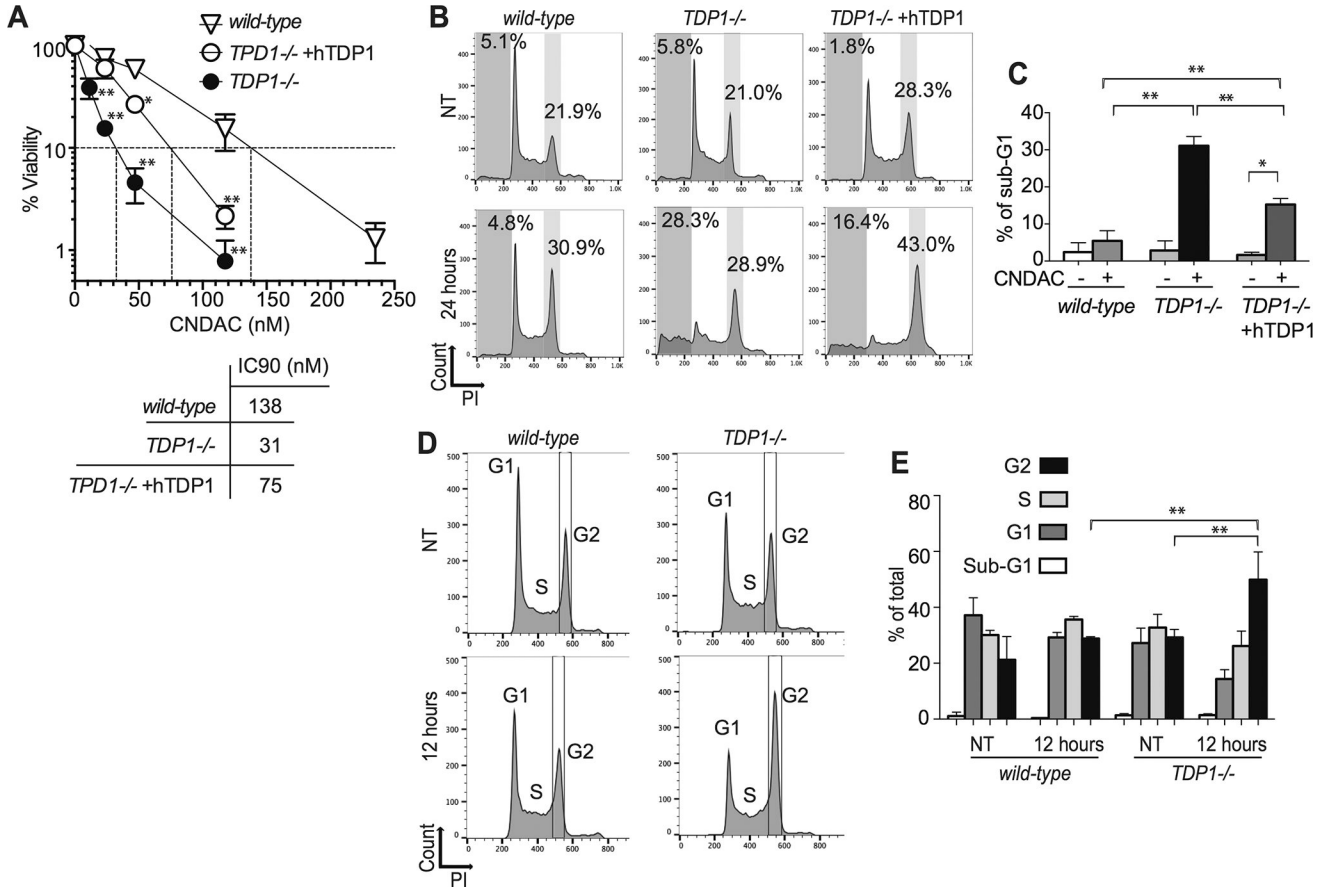

Figure 2.

Hypersensitivity of *TDP1−/−* cells to CNDAC and rescue by human TDP1. (A) Percent viability (y axis) of *wild-type* and *TDP1−/−* cells after 72 hour treatment with the indicated concentrations of CNDAC (x axis). The CNDAC IC90 is shown. Representative cell-cycle analysis of *wild-type, TDP1−/−* and *TDP1−/−* +hTDP1 cells without treatment (NT), or after 0.47 μM (B) or 0.11 μM (D) CNDAC for 24 hours. DNA content was measured by propidium iodide (PI). The percentage of sub-G1 fraction that represents the apoptotic cell fraction is shown. (C) and (E) Quantitation of experiments performed as shown in panels B and D, respectively. Error bars show the standard deviation (SD) of three independent experiments. T-test (*=p<0.05, **=p<0.001).

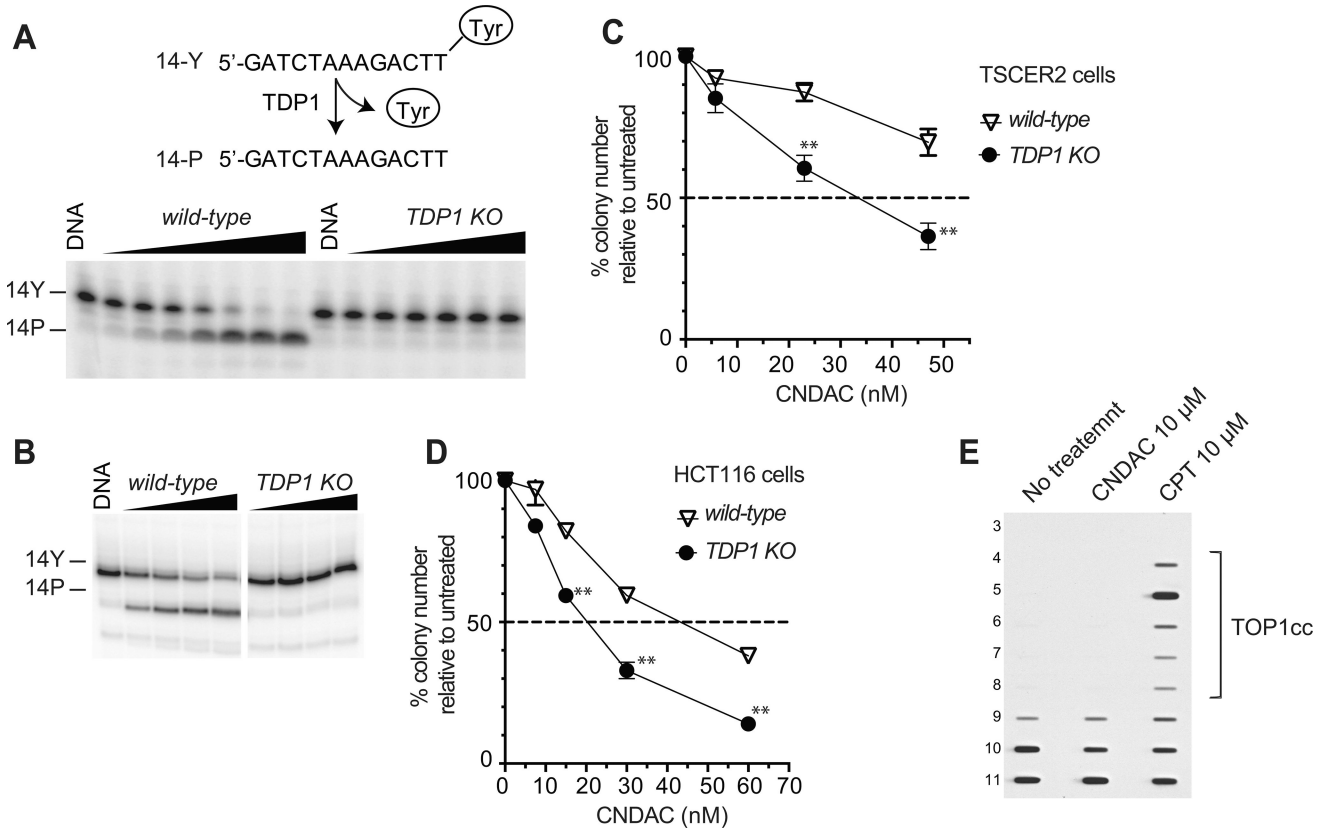

Figure 3.

Human *TDP1* knockout (*TDP1 KO*) TSCER2 and HCT116 cells are hypersensitive to CNDAC. Representative biochemical assay showing lack of TDP1 activity in the *TDP1 KO* cells. The reaction scheme is shown at the top (Tyr = 3'-phosphotyrosine). Cellular extracts from either *wild-type* or *TDP1 KO* TSCER2 (A) or HCT116 (B) cells were tested with serial dilutions (1.6, 5, 14.8, 44.4, 133, 400, 1200 μg/mL) for 30 minutes at 25°C. Reduced survival of the TDP1 KO TSCER2 (C) and HCT116 (D) cells treated with CNDAC. Y axis represents colony numbers relative to untreated cells. Cells were incubated continuously for 12 days with the indicated concentrations of CNDAC (x axis). Error bars show SD for three independent experiments. T-test (**=p<0.001). (E) Immuno Complex of Enzyme (ICE) Bioassay showing lack of TOP1cc after treatment with 10 μM CNDAC for 3 hours. 10 μM CPT for 3 hours was used as positive control (see Supplemental Figure 1 for generation of the *TDP1* knockout cell lines). Fractions 3 to 11 of total 12 fractions are shown.

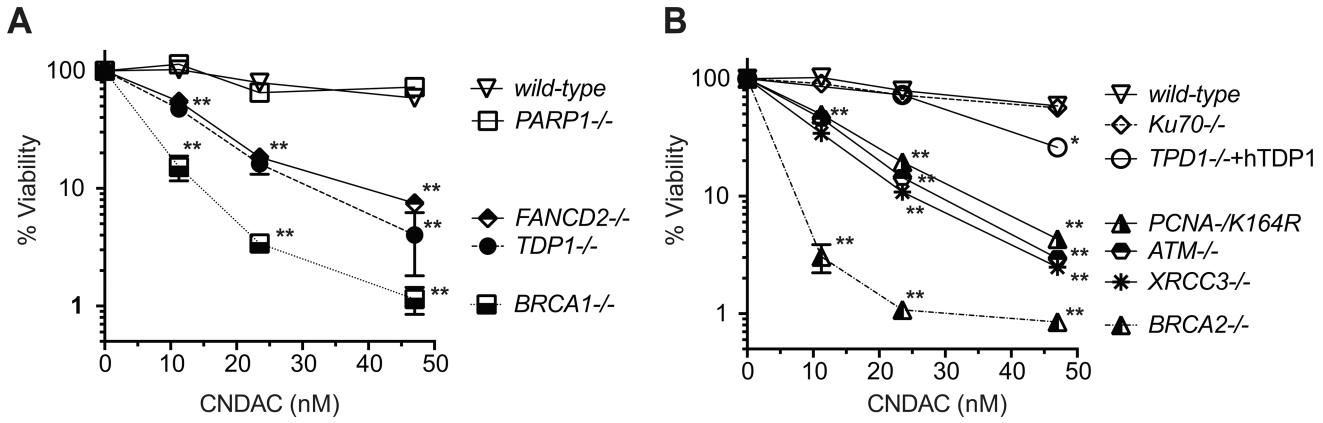

Figure 4.

Hypersensitivity of isogenic DNA repair defective DT40 cells to CNDAC. (A) and (B) Viability assays were performed as described in Figure 2. Error bars represent SD of at least 3 independent determinations. Error bars are not visible when they are encompassed within the size of the symbols. T-test (*=p<0.05, **=p<0.001). Viability curves are split in two panels (A and B) for clarity.

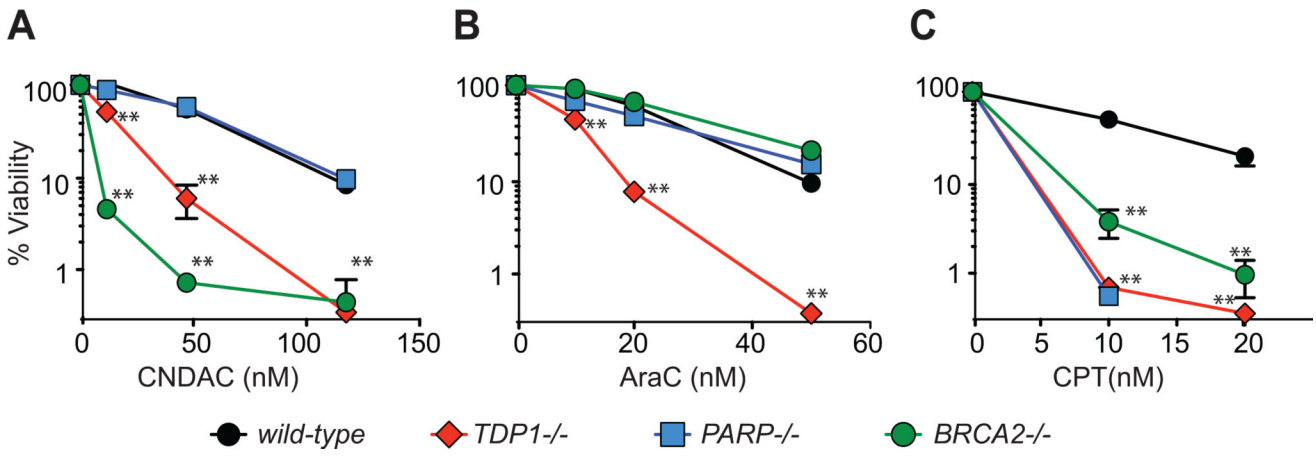

Figure 5.

Differential impact of TDP1, PARP and BRCA2 loss against representative 3'-end ssDNA lesions. The viability of the indicated DNA repair mutants after treatment with CNDAC (A), AraC (B) or CPT (C) was performed as described in Figure 1. T-test (**=p<0.001).

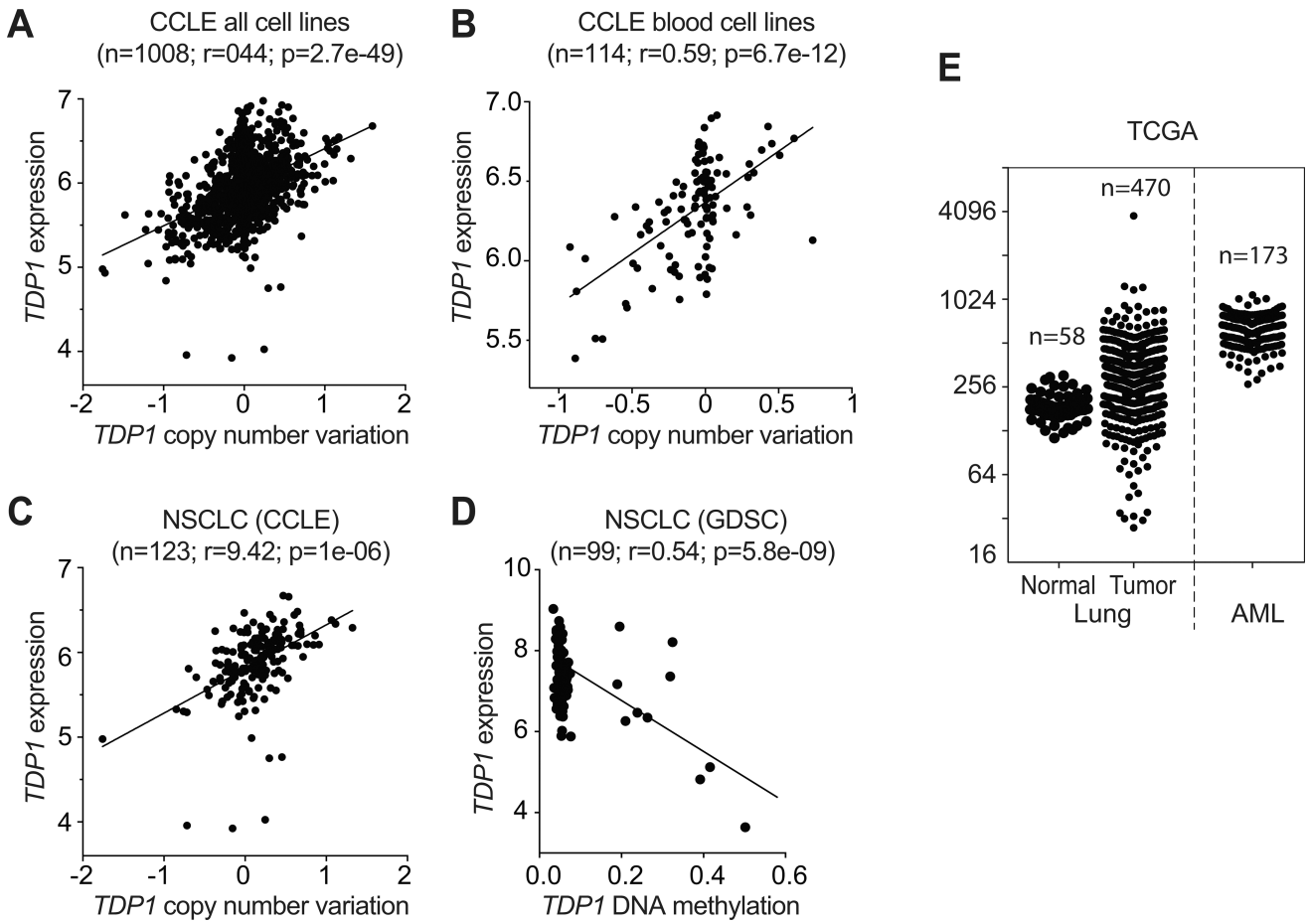

Figure 6.

TDP1 expression varies among cancer cells of the same tissue of origin as well as among cancer cells from different tissues of origin. *TDP1* messenger RNA (mRNA) (y axis, values represent log2 values) in relation to copy number variation (x axis) in the overall collection of CCLE cancer cell lines (n=1008) (A) (r=044; p=2.7e-49), in the CCLE blood cancer cell lines (n=114) (B) (r=0.59; p=6.7e-12), and in the non-small cell lung cancer cell lines (NSCLC, n=123) of the CCLE (C) (r=9.42; p=1e-06). (D) *TDP1* expression (y axis) and methylation of the *TDP1* promoter (x axis) in the NSCLC cell lines (n=99) from the GDSC database. (E) (r=0.54; p=5.8e-09). Comparison of *TDP1* expression in normal lung cells (n=58) vs NSCLC cells (n=470) and acute myeloid leukemia (AML) cells (n=173) (see Supplemental Figure 2).